CONTACTING A SINGLE C_{60} MOLECULE

C. JOACHIM[(1)], J.K. GIMZEWSK1[(2)]

(1) CEMES/CNRS
29 rue J. Marvig
31055 Toulouse Cedex
France

(2) IBM Research Division
Zürich Research Laboratory
CH-8803 Rüschlikon
Switzerland

ABSTRACT. A description of the tunneling channel through a C_{60} molecule is presented with its implications for imaging the internal structure of C_{60} using STM. The approach of an STM tip from tunneling to mechanical and electrical contact with a C_{60} molecule adsorbed on a Au(110) surface is characterized using the experimental and calculated current - distance characteristics. The term "electrical transparence" is introduced to characterize the ability of a molecule in the tip apex - surface nanoscopic cavity to participate to the electron transfer process. It is influenced both by the mechanics of the tip approach process and the modification of the electronic structure of the molecule interacting with the W tip apex and the Au(110) surface in the cavity.

1. Introduction

To be transfered from one electrode to another one via a single molecule, electrons must find favorable intramolecular tunneling channels in the molecule. These channels can be identified by measuring the resistance of the electrode-molecule-electrode junction at very low current. In the case of a single atom, the tunneling channels are non-resonant with the Fermi level of the electrodes [1,2] and result from enlargement of the width of the atomic levels due to the interaction of the atom with the electrodes [2]. For a molecule, the channels are also non-resonant [3,4]. But their identification becomes more complex as soon as the number of molecular orbitals coupled to the electrodes increases [4].

We have used a STM tip - metal surface tunnel junction to observe the consequence of a modification of the C_{60} intramolecular tunneling channels on the I(s) current-distance characteristic. The channels were modified by compressing C_{60} with the STM tip. The large deviation in I(s) characteristic observed upon compression [5] is a confirmation that the tunneling current through a molecule is controlled by the enlargement of the molecular level width due to the interaction of this molecule with the electrodes.

In section 2, the tunneling channels through C_{60} are identified for a C_{60} in equilibrium between 2 Au(110) electrodes. In Section 3, we show how these channels contribute to C_{60} images as a function of C_{60} orientation on the surface. The electrical contact and compression of C_{60} by the STM tip is discussed in section 4. In conclusion, we discuss the difference between the electrical resistance and electronic transparence of a molecule.

2. The tunneling through a single C_{60} molecule

At low bias voltage, the tunnel resistance R_t of a small metal-vacuum-metal junction can be calculated using the generalized Landauer-Büttiker formula [6]. For a small junction formed by two gold electrodes separated by 12.7 Å and with their Au(110) non-reconstructed surface 484 $Å^2$ in section, the gap resistance is $R_t = 10^{16}$ Ω. When a C_{60} molecule is introduced between the two electrodes, R_t decreases by several orders of magnitude compared to the free junction to reach 1.7×10^{8} Ω

(calculated by the elastic scattering quantum chemistry technique (ESQC) [3]. Notice that the 12.7 Å inter-electrode distance corresponds to the calculated mechanical equilibrium of the Au(110)-C_{60}-Au(110) junction [4]. The detailed variations of R_t taking into account the direct through space electrode to electrode plus the through C_{60} electron transfer processes are presented in figure 1 as a function of the electron energy. Each peak in this spectrum corresponds well to a specific set of quasi-degenerated C_{60} molecular orbitals [4].

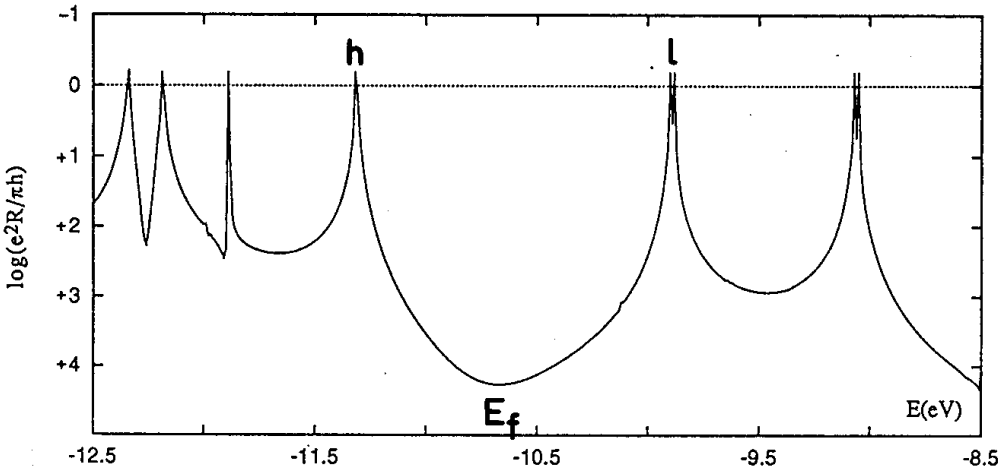

Figure 1. Variation of the tunnel resistance of the 484 $Å^2$ Au(110)-C_{60} junction as a function of the tunneling electron incident energy for a 12.7 Å inter-electrodes distance.

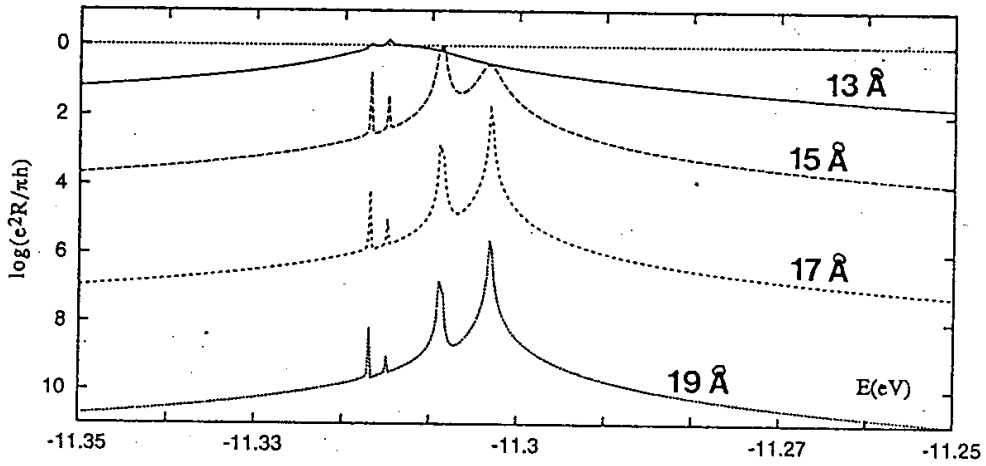

Figure 2. Variation of the tunnel resistance of a 484 $Å^2$ Au(110)-C_{60} junction as a function of the tunneling electron incident energy for different inter-electrodes distances. The energy scale is reduced compared to fig. 1 to focus on the HOMO part of the resistance spectrum.

Increasing the inter-electrode spacing and keeping C_{60} fixed in the center results in each peak remaining very narrow (figure 2). Aside from these peaks, R_t increases very rapidly but stays many orders of magnitude higher than with the free junction. Similar to the case of a single atom, the tunneling through C_{60} is non-resonant since the peak maxima are located away in energy from E_f. Each peak is the signature of the virtual resonance of a C_{60} molecular level with the electrodes.

Therefore, the tunnel current intensity near E_f through C_{60} is controlled by the coupling between the C_{60} molecular orbitals and the Au(110) surfaces. In addition, the apparent width of a given virtual resonance results not only from the coupling of a single (degenerate or not) molecular level with the electrodes: other levels, far away in energy, can contribute in a constructive or a destructive manner to its resonance tail [4]. This comes from the fact that certain levels can be more coupled to the electrodes than others. Then, the tail of their virtual resonance will extend far away in energy from their peak position. For example, 36 C_{60} orbitals are needed to recover R_t with a good approximation at E_f for a 12.7 Å inter-electrode distance: 5 HOMO, 3 LUMO and 28 others [4]. For larger inter-atomic distances, less orbitals are generaly required.

3. The C_{60} STM images

When a tip is added to one of the electrodes, the system becomes an STM junction. No deformation of C_{60} occurs under the tip when the distance between the end atom of the tip apex and the top C_{60} carbon atom is larger than the sum of their respective Van der Waals radii, i.e. around 4 Å. In this case, the coupling between C_{60} and the two electrodes (the apex and the surface) are non-symmetric. Consequently, upon tunneling on C_{60}, the tip apex will be coupled to different C_{60} molecular orbitals.

The difference between these orbitals will be imaged by the tail of the virtual resonance of the corresponding C_{60} levels as presented in figure 3. ***This implies that a C_{60} STM image does not represent the map of the electron density of a given C_{60} molecular orbital nor the C_{60} carbon atom position.*** Many molecular orbitals are mixed in a constructive or a destructive manner by their tails. This precludes the coupling of the tip with only a single molecular orbital among the 240 C_{60} ones. Furthermore, the exact molecular orbital mixing entering in the composition of an atomic orbital on a single carbon atom is rather unique. Therefore, it will be very difficult to obtain such a mixing with the virtual resonance tails coupled via the surface or via the tip. In the STM image, the overall bump shape of a C_{60} depends on a small selected number of C_{60} molecular orbitals compared to the total of 240. In contrast, the fine corrugation (i.e. the internal structure within a molecule) must be studied for each C_{60} orientation on the substrate. The mixing between the C_{60} molecular orbitals at each position of the tip apex must be decomposed orbital by orbital to explain the intramolecular corrugation contrast as recently shown using the STM-ESQC technique [4]. In Figure 4, we present experimental [7] and calculated [4] top STM images for 3 orientations of C_{60} generally found on Au(110) .

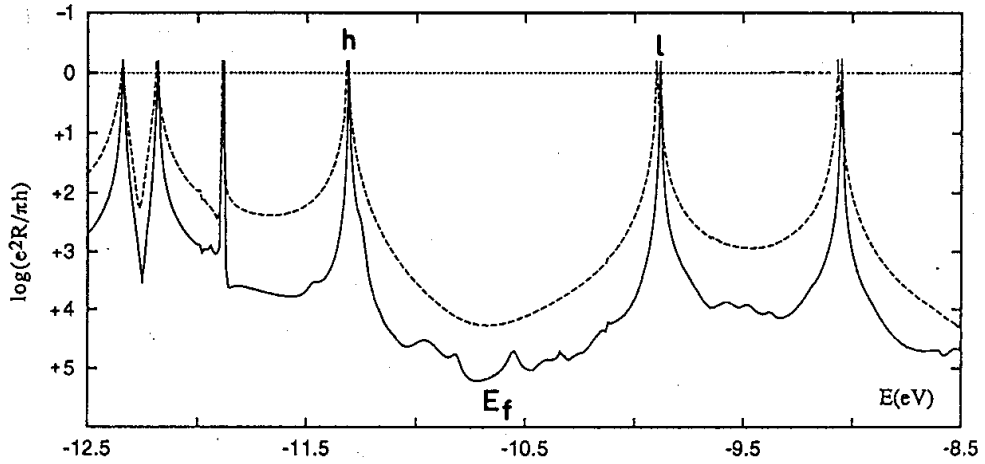

Figure 3. Variation of the resistance of a STM W tip apex-C_{60}-Au(110) surface junction as a function of the tunneling electron incident energy for a 4 Å tip apex to top C_{60} distance. For reference, the Fig. 1 spectrum is given in dash.

4. Contacting a single C_{60} molecule

To contact a single molecule with an STM, the tip must approach the molecule, but the identity of the molecule must be preserved. So, an optimum tip altitude has to be determined by measuring for example the I(s) current-altitude characteristic of the molecule concerned. C_{60} is a good candidate for such measurements since it accepts a large elastic deformation.

The experimental details are described elsewhere [5]. A STM operating at 300 K in UHV was used. 0.3 monolayer of C_{60} molecules were deposited on a Au(110) surface which creates small bidimensional C_{60} clusters shown in figure 5a. The tungsten tip was positioned on a single C_{60} in one of these clusters (figure 5b). The bias voltage was reduced to 50 mV. The tip to surface distance s was ramped and the current recorded during the ramp with the STM feedback frozen. Figure 6 presents an experimental I(s) averaged over 20 measurement and the corresponding calculated one.

For the calculation, the position of the carbon atoms of the C_{60} compressed between the W apex and the Au(110) surface was optimized using the MM2 molecular mechanic routine [8]. The constraint in this optimization was to keep the C_{60} under the tip. Molecular dynamic is not needed here since the ramp duration is longer than the relaxation time of any C_{60} vibration modes. Figure 7 presents the MM2 C_{60} mechanical energy in the junction and its radius upon compression. For each s, the tunneling current intensity was calculated with the STM-ESQC technique for the C_{60} carbon atom position optimized by MM2 and a 50 mV bias voltage.

For s > 14 Å, the junction is in a pure tunneling regime with $I(s) \propto e^{-2k_0 s}$ and $k_0 = 1.128$ Å^{-1}. The C_{60} molecular levels are enlarged by their coupling with the Au(110) surface but not mixed with the tip apex cluster orbitals. The measured and calculated k_0 lead to an apparent tunnel barrier height of $\Phi = (2k_0)^2 = 5.09$ eV on Au(110). This is very close to the averaged vacuum barrier height between an Au(110) surface ($\Phi_{Au} = 5.37$ eV) and a W tip apex with (111) facets ($\Phi_W = 4.6$ eV). Such a value is an indication that for s > 14 Å, the tunneling process through C_{60} does not change the C_{60} molecular orbitals nor their interactions with the Au(110) surface. Only the increase of the tunneling current intensity due to C_{60} introduction in the junction characterizes the mixing of the tails of the molecular level virtual resonaces. For example for s = 15 Å, $I = 5 \times 10^{-2}$ aA without a C_{60} under the tip apex and I= 1 pA with a C_{60}. k_0 is the same in both cases.

For 14 Å < s < 12 Å, the junction is in a van der Waals regime. Electrons still tunnel through C_{60} because in this regime there is only a mutual polarization of the C_{60} and tip apex electron clouds. For s= 13 Å, this leads to a small C_{60} motion upwards due to the van der Waals attraction by the tip apex (figure 6). It results a small inflection in the I(s) characteristics since the coupling between the C_{60} molecular levels and the Au(l 10) surface are weakly attenuated. This is not well reproduced by the calculation. Furthermore, C_{60} is repelled by the tip to recover conformation close to the one without the tip apex constraint (figure 7).

For 10 Å < s < 12 Å, the junction passes from a tunneling regime to a delocalization regime of the electrons between the tip apex, C_{60} and the Au(110) surface. The deformation of C_{60} lifts many of the levels degeneracy arising from a break in the symmetry of C_{60} and also because the interaction between non-consecutive carbon atoms of the C_{60} sphere increases upon compression. This level splitting is accompanied by a progressive enlargement of the width of the virtual resonances (figure 8a). The consequence is a closure of the C_{60} HOMO-LUMO gap by the anti-bonding component of the HOMO set and the bonding component of the LUMO set (figure 8b). Therefore, the resistance of the junction decreases (figure 6).

For s < 10 Å, the junction is in a conductive regime. The coupling is so intense in the cavity formed by C_{60}, the tip and the Au(110) surface that some C_{60} levels reach E_f. The resonances are then no longer virtual and the current intensity oscillates depending on which resonance is activated by the compression (figure 6). These oscillations are not observed at 300 K and the calculated resonance (figure 6) will tend to be smoothed out.

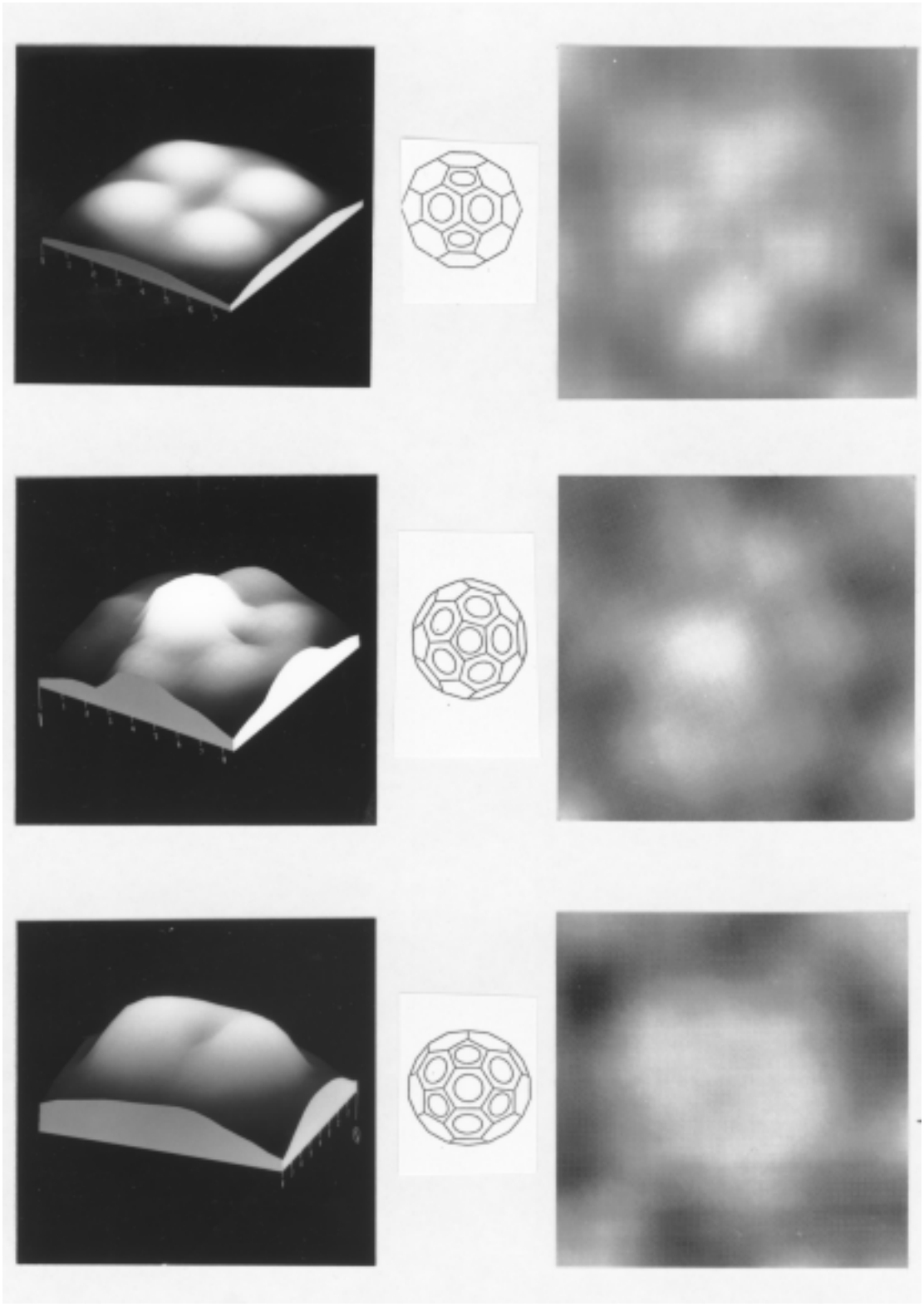

Figure 4. Experimental [7] and calculated [4] STM images of the C_{60} top for 3 C_{60} orientations on the Au(110) surface: C6-C6 for the two A6 rings, C5 for the A5 ring and C6 for the A6 ring on top.

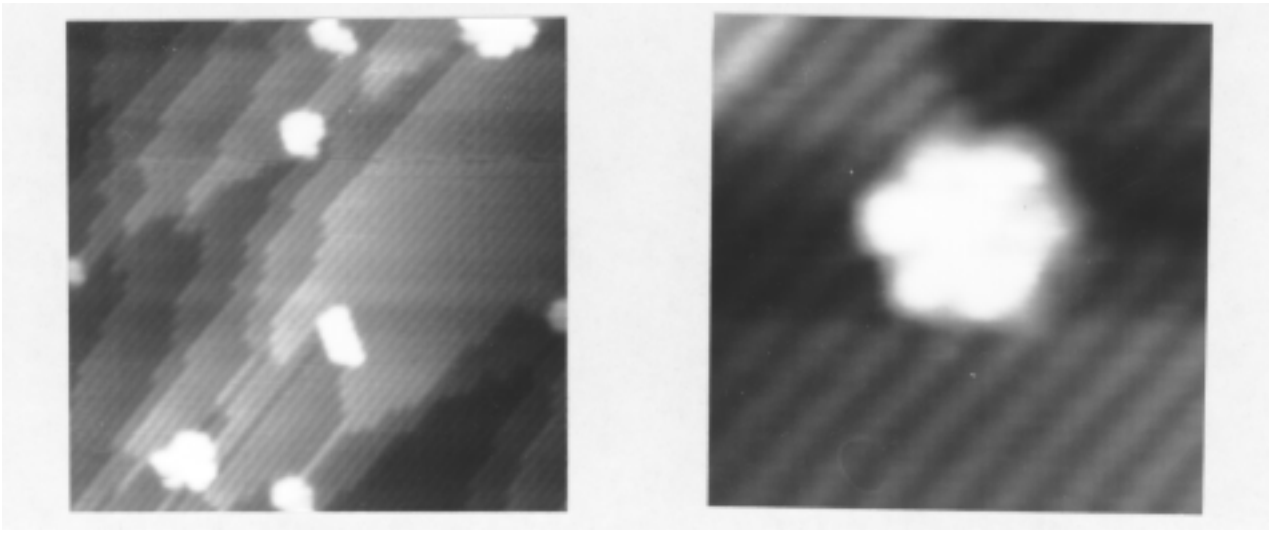

Figure 5. Experimental STM images of clusters of C_{60} molecules adsorbed on the Au(110) surface and detail of a cluster of 7 C_{60} molecules where the I(s) curve had been recorded. The Au(110) 1x2 reconstruction with a periodicity of 8.14 Å is also resolved.

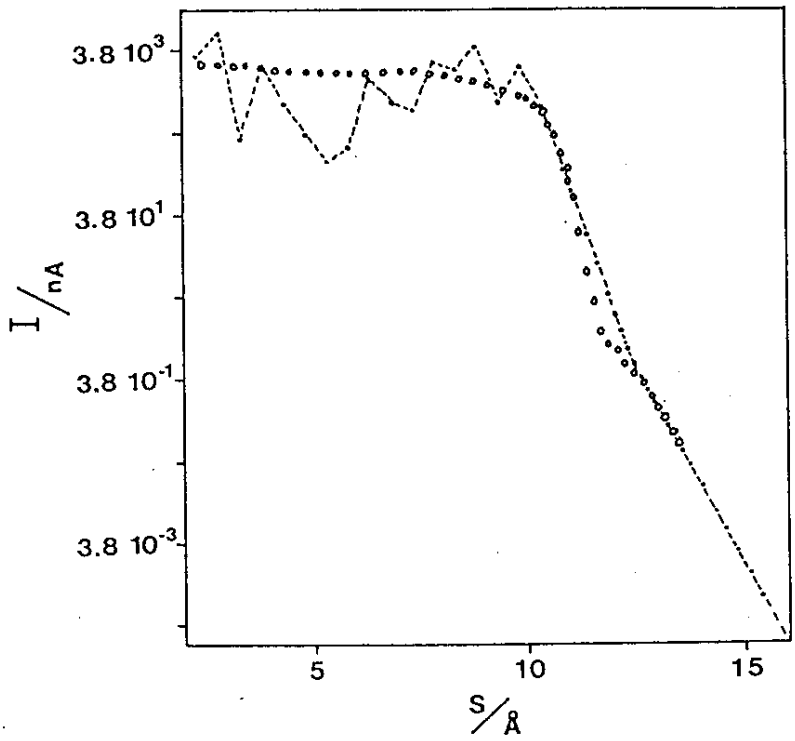

Figure 6. Experimental and calculated current-distance I(s) characteristic on a C_{60} molecule recorded at 50 mV [5].

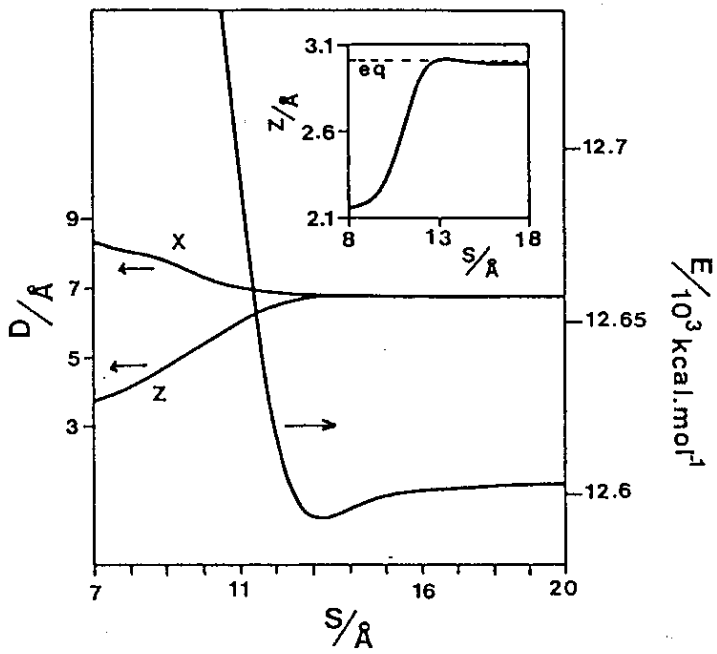

Figure 7. Calculated total C_{60} mechanical energy in the W tip apex-Au(110) surface junction as a function of the tip to surface distance. The change of the C_{60} radius (D) and the distance of the C_{60} carbon atom closest to the Au(110) surface are also given.

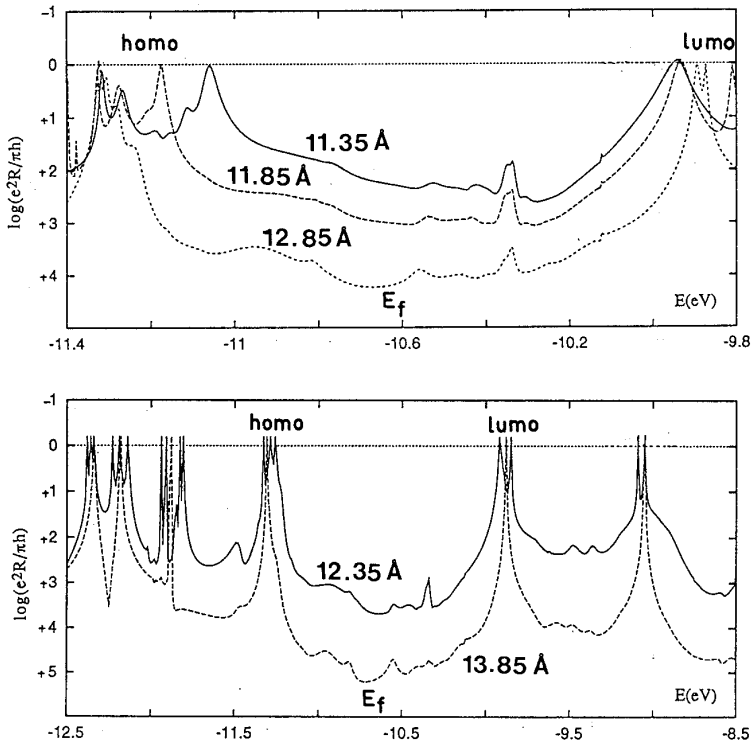

Figure 8. Variation of the resistance of the STM tunnel junction as a function of the tunneling electron incident energy for different tip apex to surface distance. The total deformation of the tip apex was taken into account in the resistance calculation. The tip apex to surface distances chosen for the C_{60} conformation optimization under the tip before the tunnel current calculations are indicated on each resistance spectrum.

5. The electrical transparence of C_{60}

An electrical contact is made on a material if a large current can flow through it for a minimum transformation of the sample. The C_{60} energy variations in the junction (figure 6) indicates that around s = 12.0 Å, the attractive part of the C_{60}-apex interaction is compensated by the repulsive part and that C_{60} recovers approximately its free shape. This corresponds also to a change in the log(I) slope. Then, for s around 12.0 Å, the current intensity is maximized for a minimum deformation of C_{60} and the tip-C_{60}-Au(110) junction resistance is R_t = 54.807 MΩ.

Since the experimental and the calculated I(s) are very closed, the R_{C60} resistance can be estimated using the generalized Büttiker-Landauer formula [6]. Substracting the constriction resistance from R_t leads to R_{C60} = 54.794 MΩ. Care must be taken on the signification of this resistance [5]. The electric resistance of a single molecule must characterize the loss of energy of the electrons flowing through this molecule. But there is no dissipation included in the Büttiker-Landauer formula [9]. Moreover, dissipation effects are certainly accounted in the 54.807 MΩ experiental junction resistance. We have no means yet to extract them to date.

Therefore, what is measured by R_{C60} is the electronic transparence t/r of a C_{60} at E_f when adsorbed on a Au(110) surface with $R_t = R_0 (1+r/t)$, $R_0 = h/2e^2$ and t the monoelectronic transmission coefficient (the transmittance) of a Bloch wave elastically scattered by the junction. From figure 6, the C_{60} electronic transparence is $t/r = 2.35 \times 10^{-4}$. We have shown in section 2 and 4 that the finite R_t value at E_f is due to the enlargement and the shift of the C_{60} level virtual resonances reaching E_f by their tails. Therefore, this electronic transparence is not only an intrinsic characteristic of a molecule but characterizes also the coupling between the molecule and the electrodes.

6. Acknowledgements

We wish to thank C. Chavy, R. Berndt and R.R. Schlitter for usefull discussions. This work was supported partially by the BBW switzerland under the Esprit 'PRONANO' project n° 8523.

7. References

1. D. Eigler, P.S. Weiss, E.K. Schweizer, N. Lang, Phys. Rev. Lett., 66, 1189 (1991).

2. X. Bouju, C. Joachim, C. Girard and P. Sautet, Phys. Rev. B, B47, 7474 (1993).

3. P.Sautet and C. Joachim, Chem. Phys. Lett., 185, 23 (1991).

4. C. Chavy, C. Joachim and A. Altibelli, Chem. Phys. Lett., 214, 569 (1993).

5. C. Joachim, J.K. Gimzewski,R.R. Schlittler, C. Chavy, Phys. Rev. Lett., submitted (1994).

6. R. Landauer, J. Phys. C, 1, 8099 (1989).

7. R. Gaisch, R. Berndt, J.K. Gimzewsky, B. Reihl, R.R. Schlittler, W.P. Schneider, M. Tschudy, Appl. Phys. A, 57, 207 (1993).

8. N.L. Allinger, R.A. Kuk, M.R. Iman, J. Com. Chem., 9, 591 (1988).

9. C. Joachim, New J. Chem., 15, 223 (1991).